Near-Edge X-ray Absorption Fine Structure of DNA Nucleobases Thin Film in the Nitrogen and Oxygen K-edge Region

K. Fujii,[†] K. Akamatsu,[‡] and A. Yokoya[†]

Synchrotron Radiation Research Center, Japan Atomic Energy Research Institute, SPring-8, 1-1-1 Koto, Mikazuki, Sayo, Hyogo 679-5148, Japan and Radiation Risk Analysis Laboratory, Japan Atomic Energy Research Institute, 2-4 Shirakarashirane, Tokai, Naka, Ibaraki, 319-1195, Japan

Received: September 26, 2003; In Final Form: February 20, 2004

The near-edge X-ray absorption fine structure (NEXAFS) of evaporated thin films of DNA nucleobases on an Au-coated Si surface at room temperature has been investigated in the regions around the nitrogen and oxygen K-edges using highly monochromatic synchrotron soft X-rays. Each nucleobase shows a specific absorption spectrum originating from the resonant excitation of 1s electrons of nitrogen or oxygen to antibonding states, some of which strongly depend on the polarization angle of incident soft X-rays. From an analysis of the polarization angle dependences of the π^* resonance absorption intensity, it is found that purines are orientated to the multilayer surface with an angle of $15 \pm 6°$ for adenine and $38 \pm 1°$ for guanine. Uracil has an orientation of $16 \pm 4°$, although other pyrimidines such as thymine and cytosine are randomly orientated with respect to the surface. These characteristics of the obtained NEXAFS spectra not only reveal the electrical structure of the nucleobases but also provide us with knowledge of the thermal stability of the self-organized base-stacking structure, which might play an important role in retaining the conformation of an intact or base-damaged DNA molecule.

1. Introduction

Exploring the electronic states of biological molecules is essential to understanding the interaction between molecules and photons or charged particles in tracks of ionizing radiation.[1] Using the concept of optical approximation, the excitation or ionization intensity of a molecule interacting with charged particles can be predicted as a distribution of the oscillator strength of the molecule.[2,3] The oscillator strength is strongly related to optical constants such as the photoabsorption cross section (see review 4). Therefore, measuring such optical parameters for biological molecules, which interact with radiation, is indispensable not only to understanding of the resulting physicochemical process of the chemical molecular damage but also to providing parameters for track-simulation studies of biological systems.

The first target of radiation impact in a living cell is the DNA molecule (see reviews 5 and 6). Several studies have been performed to measure the photoabsorption spectrum in the energy region corresponding to secondary electrons generated at the end of a radiation track. Inagaki and co-workers have reported the photoabsorption spectrum of DNA around the first ionization potential in the ultraviolet region (>100 eV) using a photoacoustic method.[7] Above 0.1 keV, there are the K-edges of carbon, nitrogen, oxygen, and phosphorus (280, 400, 530, and 2150 eV, respectively), which are the basic constituents of DNA. Recently, this energy region has been highlighted because the secondary electrons in this region cause relatively denser ionization/excitation than higher-energy radiation such as γ-rays and in turn induce local multiple damage to DNA[8,9] Kirtley and co-workers have revealed that the fine structure of the photoabsorption spectrum of DNA around the nitrogen K-edge strongly depends on the chemical circumstances of the nitrogen atom in DNA.[10] It is generally known that such an absorption structure around the K-edge, called NEXAFS (near-edge X-ray absorption fine structure), has a large photoabsorption cross section, even though below the ionization potential of the K-shell electron to the continuum level there is a so-called giant π^* resonance peak. However, there have been very few studies attempting to assign the electronic states of the fine structure. Mochizuki and co-workers have used Hartree−Fock static exchange (HF−STEX) calculations to theoretically calculate the transition energy from nitrogen 1s to a π^* excitation for purine bases only (adenine and guanine).[11]

In the present study, we experimentally measured NEXAFS spectra for evaporated DNA nucleobase (adenine, guanine, thymine, and cytosine) films as well as for films of chemically modified bases (uracil and 5-halouracil). On the basis of the obtained NEXAFS spectra, the electronic states of the fine structure in each spectra were assigned by calculating the molecular orbitals. By further analysis of the dependence of the π^* resonance absorption intensity on the polarization angle of incident soft X-rays, we also discuss the self-organized base-stacking structure on the sample surface.

2. Materials and Methods

Nucleobase (adenine (A), guanine (G), cytosine (C), and thymine (T)) powders were purchased from Tokyo Kasei Ltd, uracil (U) and 5-halouracils (5-fluorouracil (FU), 5-chlorouracil (ClU), 5-bromouracil (BrU), and 5-iodouracil (IU)) were purchased from Sigma Aldrich and used without further purification. Each molecular structure is shown in Figure 1. The nucleobases were evaporated onto a Au-coated Si surface (10×5 mm^2) using a miniature oven in a vacuum to obtain thin films of the bases. The quantity of the evaporated sample was monitored using a deposition monitor (CRTM-6000; ULVAC Ltd.). The evaporation rate was below 2 nm/sec, with the monitor and the sample positioned at the same distance from

* Address correspondence to this author. E-mail: fujiken@spring8.or.jp.
[†] Synchrotron Radiation Research Center.
[‡] Radiation Risk Analysis Laboratory.

10.1021/jp036872f CCC: $27.50
Published on Web 05/12/2004

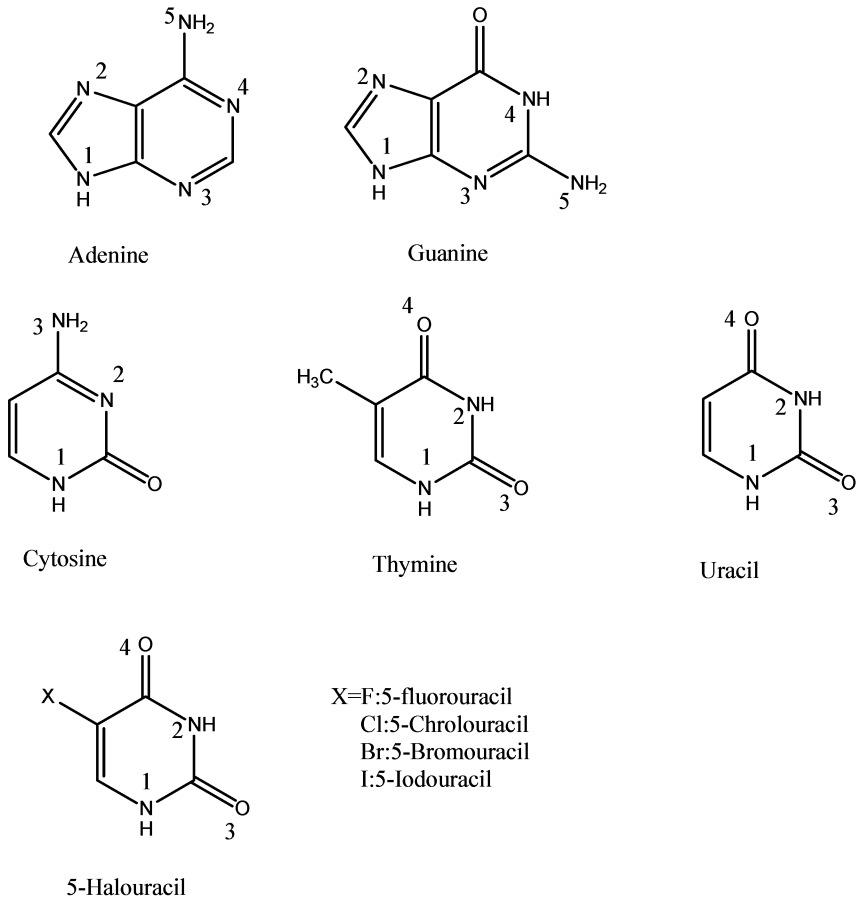

Figure 1. Molecular structures of nucleobases and 5-halouracil with the nitrogen atoms in each nucleobase numbered. The letter X in the 5-holouracil structure refers to halogenation with F:fluoro-, Cl: chloro-, Br:bromo-, and I:iodo-.

the oven, to obtain a thickness of ~100 nm. The purity of the sample was checked by an HPLC method after recovery from the surface, and no detectable degradation was observed after evaporation.

Samples were placed into a load-lock chamber ($<10^{-4}$ Pa) for degassing for a few tens of minutes and then transferred to an ultrahigh vacuum chamber ($<10^{-6}$ Pa) for X-ray absorption measurements. X-ray absorption measurements were carried out at the JAERI soft X-ray beamline (BL23SU) in SPring-8 using the circularly polarized light mode.[12] We measured the drain current from the sample (I) and that from the post focus mirror (I_M) with two electrometers (TR8652, Advantest Co.) and obtained the normalized intensity (I/I_M), which is proportional to the photoabsorption coefficient. We observed the values of the intensity as a function of photon energy and obtained the NEXAFS spectrum. The effect of contaminants on the mirror was insignificant in the I_M spectra. The resolution of the monochromator ($\Delta E/E$) was estimated to be ~0.2 eV at 400 eV and ~0.3 eV at 530 eV for the measurement condition. The angle between the electric field (E) vector of the synchrotron soft X-rays and the normal to the surface of the sample was changed from 30° to 90°. All measurements were performed at room temperature. The absolute photon energy was calibrated by measuring the binding energy of the Au 4f photoelectron using a hemispherical electron analyzer installed on the same beamline.

3. Results

3.1. Nitrogen 1s NEXAFS Spectra. Figure 2a−e shows the N 1s NEXAFS spectra for A, G, C, T, and U thin films, respectively, as a series of angles (θ) between the E vector of the incident photon and the surface normal. These spectral structures are quite consistent with the previous structures reported by Kirtley et al.[10] Roughly, their spectra can be divided into two regions; one is consistent with strong and fine structure in the lower-energy region and the other with relatively broad peaks in the higher-energy region. We have recently found[13] that 1s to π^* resonance peaks exist in the lower-energy region (398−404 eV at the nitrogen K-edge, 530−532 eV in the oxygen K-edge). In addition, π^* resonance peaks form discrete and sharp structures in the spectrum, but σ^* peaks form a broad structure in the higher-energy region compared to the π^* resonance peak region. Rydberg states and multielectron excitations might be superimposed on the broad peaks starting from 405 eV in the nitrogen K-edge region and from 535 eV for that of oxygen. We assigned the nitrogen 1s to π^* resonant excitation energy of each of the nucleobases (Table 1) by deconvoluting the NEXAFS spectrum into Gaussian, asymmetric Gaussian, and error functions for π^*, σ^*, and edge jump, in considering the above issues (Figure 3). The ionization potential of each molecule was estimated from the results of curve fitting using a least-squares method.

In the NEXAFS spectra of A, G, and U, the intensities of the π^* resonance are larger than or comparable to those of the σ^* resonance at grazing incidence (small θ). As θ increases, the intensities of the π^* resonance become smaller than those of the σ^* resonance. These phenomena also occur in the O K-edge region (mentioned in Section 3.2 below). These results indicate that the local structures representing the π^* resonance have some orientations in the A, G, and U thin films. In contrast, the π^* peak intensities have no E vector angle dependency in

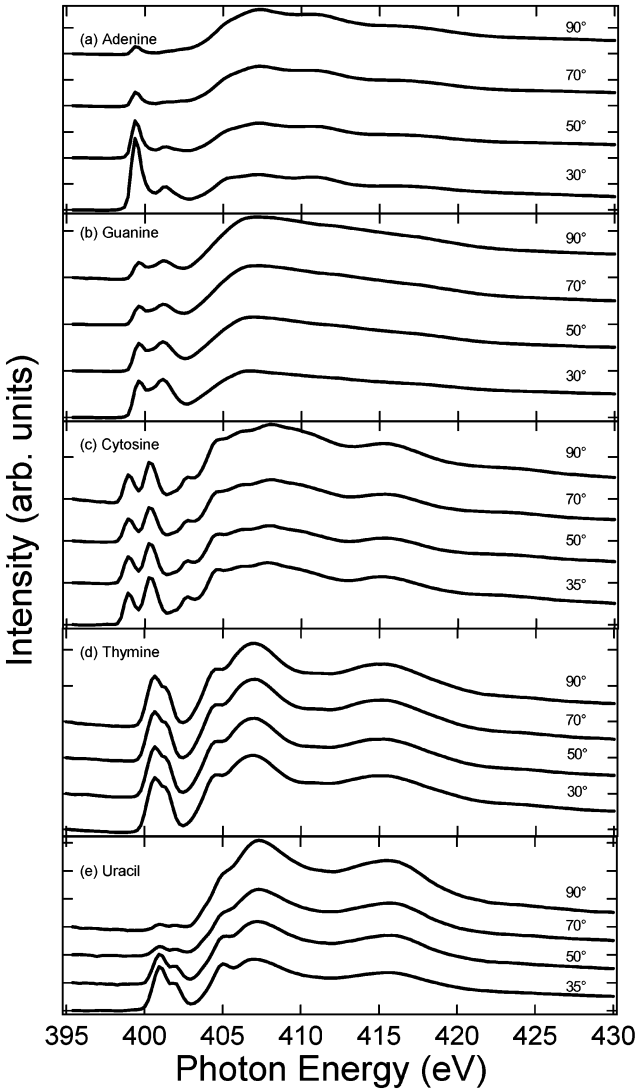

Figure 2. NEXAFS spectra of nucleobase thin films around the nitrogen K-edge region of (a) adenine, (b) guanine, (c) cytosine, (d) thymine, and (e) uracil. From bottom to top, the curves show the results at polarization angles of $\theta = 30-90°$.

the T and C NEXAFS spectra, indicating that T and C pyrimidine are randomly orientated with respect to the surface. We chose vector type π^* peaks to analyze the angular dependence of the NEXAFS spectrum. Equation 1 holds for the analysis of the angular dependence of this π^* orbital.[14] The angle-dependent transition intensity of the π^* resonance is expressed as follows:[14]

$$I(\theta) = A\left\{\frac{P}{3}\left[1 + \frac{1}{2}(3\cos^2\theta - 1)(3\cos^2\alpha - 1)\right] + \frac{(1-P)}{2}\sin^2\alpha\right\} \quad (1)$$

where P is the degree of linear polarization of the X-rays ($P = 0.5$ because of the circular polarization used here), A is the constant describing the angle-integrated cross section, and α is the polar angle between the surface normal and the vector of the π^* molecular orbital. The best-fit value of α was determined so as to perform a nonlinear least-squares routine using eq 1 (Figure 4). We obtained the value of $\alpha = 15 \pm 6°$ for A, $38 \pm 1°$ for G, and $16 \pm 4°$ for U. To examine the effects of structural hindrance on the orientation originating from a functional group

TABLE 1: Excitation Energies (in eV) from Nitrogen 1s to π^*

initial state	adenine	guanine	cytosine	thymine	uracil
N1	404.1 (404.1)[a]	401.3 (404.3)	400.4	401.5	401.9
N2	399.8 (401.4)	399.5 (401.5)	398.9	400.7	400.9
N3	399.3 (401.2)	400.6 (402.3)	402.8		
N4	399.8 (401.4)	401.3 (404.3)			
N5	401.2 (403.5)	403.4 (404.8)			

[a] The values in brackets show the theoretical values from ref 11.

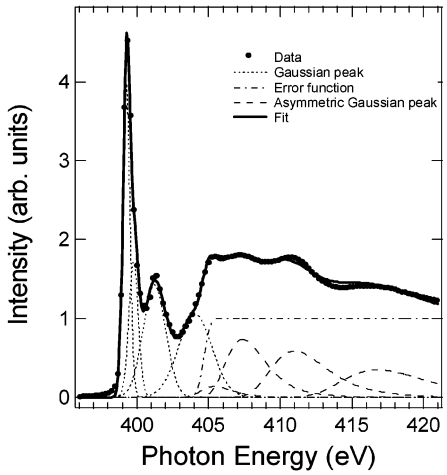

Figure 3. Typical least-squares fits of NEXAFS of adenine in the N K-edge region. The fitting routine was based on fitting the data with the sum of a number of Gaussian peaks, asymmetric Gaussian peaks, and an error function.

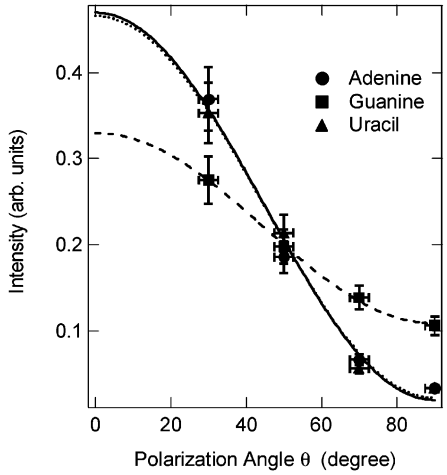

Figure 4. Polarization dependence of the intensities of the π^* resonances in the N 1s NEXAFS spectra of nucleobases. The symbols (●■▲) show the normalized peak area ratios of the lowest π^* resonance of adenine, guanine, and uracil obtained from the curve-fitting procedure. Solid, dashed, and dotted lines show the curve fitting results for A, G, and U, respectively.

located on the pyrimidine ring, we also tested for 5-halouracil (FU, ClU, BrU, and IU). From the same analysis as that described above, all the 5-halouracil thin films showed specific orientation with respect to the surface (α for F: $20 \pm 13°$, ClU: $32 \pm 6°$, BrU: $29 \pm 2°$, and IU: $32 \pm 4°$) (Figure 5). The NEXAFS spectrum did not show any dependence on the azimuthal angle of the sample with respect to the electric field vector of the incident soft X-rays.

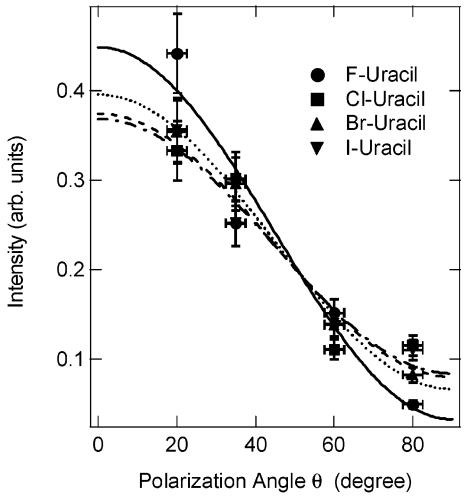

Figure 5. Polarization dependence of the intensities of the π^* resonances in the N 1s NEXAFS spectra of 5-halouracils. The symbols (●■▲▼) show the normalized peak area ratios of the lowest π^* resonance of FU, ClU, BrU, and IU obtained from the curve-fitting procedure. Solid, dashed, dotted, and dashed-and-dotted lines show the curve-fitting results for FU, ClU, BrU, and IU, respectively.

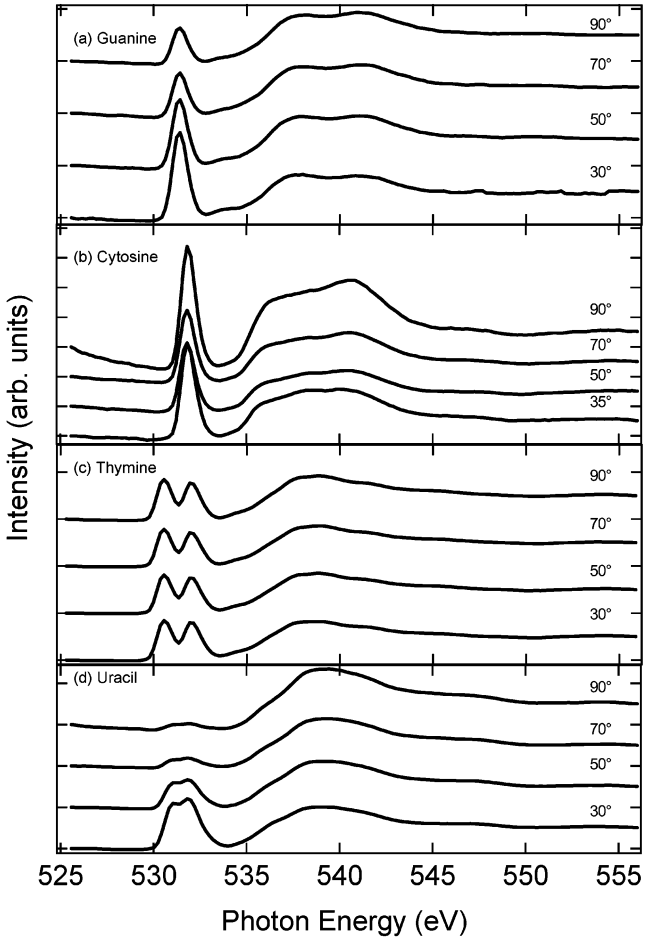

Figure 6. NEXAFS spectra of nucleobase thin films around the oxygen K-edge region of (a) guanine, (b) cytosine, (c) thymine, and (d) uracil, respectively. From bottom to top, the curves show the results at the polarization angles $\theta = 30-90°$.

3.2. Oxygen 1s NEXAFS Spectra. Figure 6a−d shows the O 1s NEXAFS spectra for G, C, T, and U thin films, respectively. Adenine has no spectral structure in this region because of the lack of an oxygen atom in the molecule. These spectra can also be divided into two regions, namely, the π^* and σ^* excitation regions as seen in the N K-edge NEXAFS spectra (see above). In the oxygen K-edge NEXAFS spectra, there are π^* peaks around 530−532 eV and σ^* peaks around 532−550 eV. From the same analysis as that described above, G and U were orientated at 38 ± 1° and 16 ± 4°, and all the 5-halouracil thin films are orientated with respect to the surface (α for F: 29 ± 5°, ClU: 23 ± 16°, BrU: 23 ± 5°, and IU: 33 ± 3°), to which C and T are randomly orientated (Figures 7 and 8). This orientation indicates the tilt angle of the π^* (C═O) molecular orbital. The results obtained from curve-fitting by the same method described above suggest π^* resonance peaks in the oxygen K-excitation region, as listed in Table 2. The NEXAFS spectrum did not show any dependence on the azimuthal angle of the sample with respect to the electric field vector of the incident soft X-rays.

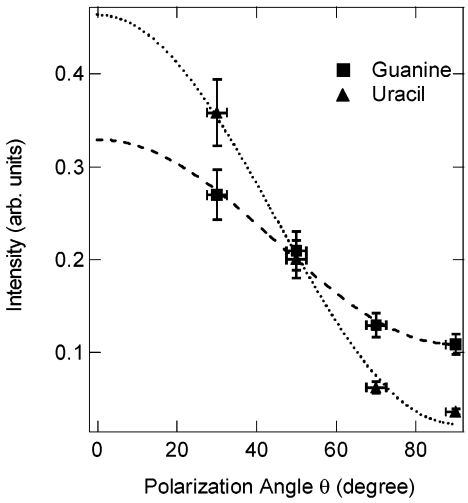

Figure 7. Polarization dependence of the intensities of the π^* resonances in the O 1s NEXAFS spectra of nucleobases. (■▲) show the normalized peak area ratios of the lowest π^* resonance of G and U obtained from the curve-fitting procedure. Dashed and dotted lines show the curve-fitting results for G and U, respectively.

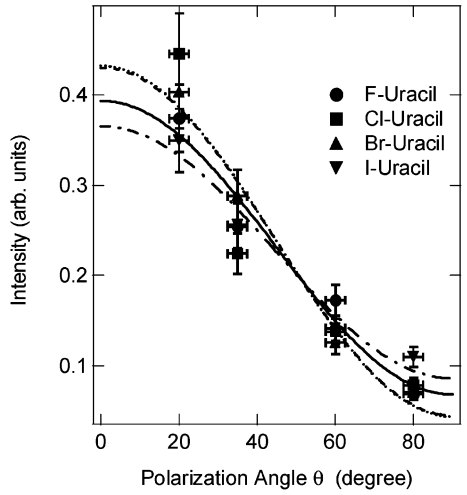

Figure 8. Polarization dependence of the intensities of the π^* resonances in the O 1s NEXAFS spectra of 5-halouracils. (●■▲▼) show the normalized peak area ratios of the lowest π^* resonance of FU, ClU, BrU, and IU obtained from the curve-fitting procedure. Solid, dashed, dotted, and dashed-and-dotted lines show the curve-fitting results for FU, ClU, BrU, and IU, respectively.

4. Discussion

The role of core-level photoabsorption in the constituent atoms of DNA, namely, carbon, nitrogen, and oxygen, has been

TABLE 2: Excitation Energies (in eV) from Oxygen 1s to π^*

initial state	guanine	cytosine	thymine	uracil
O	531.4	531.9		
O3			532.0	531.9
O4			530.5	530.9

discussed with respect to the cell-killing effect of heavy-ion beam irradiation on living cells.[15] To date, many studies have tried to provide an outline of the K-shell photoabsorption effect on radiation damage to DNA such as DNA strand breaks using monochromatic soft X-rays.[16−18] These studies, however, were performed without any knowledge of the fine structure in the photoabsorption spectrum generally appearing around the K-edge region. A lack of knowledge regarding the precise photoabsorption cross sections, which are obtained as a near-edge X-ray absorption fine structure (NEXAFS) spectrum of a target DNA molecule, tends to lead to an erroneous estimation of the absorbed dose because, in general, the cross sections at the π^* and σ^* resonances greatly differ from those at energies wholly above the ionization potential.

NEXAFS data for organic and inorganic molecules have been tabulated by Hitchcock;[19] for DNA molecules, however, data have been very scarce except for those obtained from several experimental studies[10,13] and, to our knowledge, one theoretical study.[11] In the present study, we obtained the NEXAFS spectra of a series of DNA nucleobases in the energy region around the nitrogen and oxygen K-edges. All the bases tested in this study showed a characteristic resonant excitation structure originating from a 1s electron of nitrogen or oxygen excited into unoccupied orbitals, namely, the π^* and σ^* orbitals. Each π^* resonant energy level is successfully assigned by deconvoluting the obtained spectra using Gaussian peaks, asymmetric Gaussian peaks, and the error function. The knowledge obtained regarding the core-level excitation energies and the cross sections for the nucleobases will be important for studying the collision processes between charged particles and DNA.

We have also shown that the photoabsorption intensity of each nucleobase depends on the polarization angle of the electric field vector of the incident photon. By analyzing the detail of these relationships, we estimated the tilt angle of the nucleobases arranged on the surface. The molecular planes of U and FU are tilted approximately 20 degrees from the surface. ClU, BrU, and IU are tilted approximately 30 degrees. It is inferred that these molecules are not bent because all the intensity of the nitrogen π^* peaks showed the same angular dependence in each spectrum. Analysis of the oxygen π^* peaks shows that the angles between the C═O bonds and the surface are the same as those between the molecular planes and the surface. T and C, on the other hand, show a constant value for the π^* resonance peak intensity as the polarization angle of the incident photon is changed. These results indicate that both nucleobases have isotropic adsorption structures on the surface. The van der Waals radius of the methyl group, which is one of the functional groups in thymine (2.0 Å),[20] is nearly identical to those of Cl, Br, and I atoms (1.80, 1.95, and 2.15 Å, respectively).[20] This similarity indicates that the steric hindrance of the functional group located outside of the pyrimidine ring is not the only thing preventing the molecule from being arranged and layered on the surface.

Recently, Furukawa and co-workers have applied an STM method to observe the formation of a submonolayer surface of nucleobase molecules adsorbed on a Cu(111) substrate.[21,22] They concluded that a specific dimer of the nucleobases formed by hydrogen bonds forms a two-dimensional self-assembled structure of DNA base molecules on the surface. However, it is difficult to precisely compare the mechanisms between the submonolayer surface and the condensed film of the present study, as the latter was deposited more rapidly (∼2 nm/s) than the former (∼1 molecule/min).[22] The van der Waals force, which is induced by the dipole−dipole interaction or the dispersion force in addition to the hydrogen-bonding force and the electromagnetic force created by the π-electron, significantly contributes to forming the physisorption structure, the stacking structure of DNA nucleobases, and the molecular orientated structure.[23,24] It is, therefore, inferred that van der Waals forces also contribute to forming the self-assembled molecular layer in the condensed molecules. Functional groups such as the methyl- or amino-groups in T and C might affect the interaction mediated by the force between the molecules, causing isotropic adsorption structures to appear in the multilayer structure of T and C.

Conclusion

The NEXAFS spectrum not only provides us with information regarding the lowest unoccupied molecular orbital of the molecule but also demonstrates aspects of the self-assembling molecular stacking structure. It is considered that this self-assembled structure composed of nucleobases plays an important role in forming the tertiary structure of a DNA molecule including normal or damaged nucleobases.

Acknowledgment. We would like to thank Dr. Agui and Dr. Yoshigoe (JAERI, SPring-8) for operating the beamline.

References and Notes

(1) *Symposium on Radiobiology. The Basic Aspects of Radiation Effects on Living Systems;* Nixon, J. J., Ed.; Wiley: New York, 1952; p 153.
(2) Platzman, R. L. *Vortex* **1962**, *12*, 372−389.
(3) Fano, U. *Radiat. Res.* **1975**, *64*, 217−232.
(4) Hatano, Y. *Phys. Report* **1999**, *313*, 109−169.
(5) O'Neill, P.; Fielden, E. M. *Adv. Radiat. Biol.* **1993**, *17*, 53−120.
(6) Becker, D.; Sevilla, M. D. *Adv. Radiat. Biol.* **1993**, *17*, 121−180.
(7) Inagaki, T.; Hamm, R. N.; Arakawa, E. T. *J. Chem. Phys.* **1974**, *61*, 4246−4250.
(8) Goodhead, D. T. *Int. J. Radiat. Biol.* **1994**, *65*, 7−17.
(9) Ward, J. F. *Int. J. Radiat. Biol.* **1994**, *66*, 427−432.
(10) Kirtley, S. M.; Mullins, O. C.; Chen, J. E.; George, S. J.; Chen, C. T.; O'Halloran, T.; Cramer, S. P. *Biochim. Biophys. Acta.* **1992**, *1132*, 249−254.
(11) Mochizuki, Y.; Koide, H.; Imamura, T.; Takemiya, H. *J. Synchrotron Radiat.* **2001**, *8*, 1003−1005.
(12) Saitoh, Y.; Nakatani, T.; Matsushita, T.; Agui, A.; Yoshigoe, A.; Teraoka, Y.; Yokoya, A. *Nucl. Inst. Methods in Phys. Res. A* **2001**, *474*, 253−258.
(13) Fujii, K.; Akamatsu, A.; Muramatsu, Y.; Yokoya, A. *Nucl. Instrum. Methods Phys. Res., Sect. B* **2003**, *199*, 249−254.
(14) *NEXAFS Spectroscpy*; Stöhr, J., Ed.; Springer: Berlin, 1992; Vol. 25, p 276.
(15) Chetioui, A.; Despiney, I.; Guiraud, L.; Adoui, L.; Sabatier, L.; Dutrillaux, B. *Int. J. Radiat. Biol.* **1994**, *65*, 511−522.
(16) Fayard, B.; Touati, A.; Abel, F.; Herve du Penhoat, M. A.; Desiney-Bailly, I.; Gobert, F.; Ricoul, M.; L'Hoir, A.; Politis, M. F.; Hill, M. A.; Stevens, D. L.; Sabatier, L.; Sage, E.; Goodhead, D. T.; Chetioui, A. *Radiat. Res.* **2002**, *157*, 128−140.
(17) Goodhead, D. T.; Thacker, J.; Cox, R. *Phys. Med. Biol.* **1981**, 1115−1127.
(18) Yokoya, A.; Watanabe, R.; Hara, T. *J. Radiat. Res.* **1999**, *40*, 145−158.
(19) Hitchcock, A. P.; Mancini, D. C. *J. Electron. Spectrosc.* **1994**, *67*, 1−132.
(20) Pauling, L. *The Nature of the Chemical Bond*, 1960.
(21) Furukawa, M.; Tanaka, H.; Kawai, T. *J. Chem. Phys.* **2001**, *115*, 3419−3423.
(22) Kawai, T.; Tanaka, H.; Nakagawa, T. *Surf. Sci.* **1997**, *386*, 124−136.
(23) Israelachvili, J. N. *Intermolecular and Surface Forces;* Academic Press: London, 1985.
(24) Saenger, W.; *Principles of Nucleic Acid Structure*; Springer: Berlin, 1984.